Performance of High-Angle Time Projection Chambers in the T2K Near Detector Upgrade

Merlin Varghese
Institut de Física d'Altes Energies (IFAE)
Barcelona, Spain
mvarghese@ifae.es
On behalf of the T2K ND280 TPC Group

09/07/2025
EPS-HEP Conference 2025, Marseille

Outline

1. Introduction: The T2K experiment and Near Detector Upgrade
2. High Angle Time Projection Chambers (HA-TPC)
3. Performance of HA-TPCs
4. Future Prospects
5. Summary

Tokai to Kamioka(T2K) Experiment

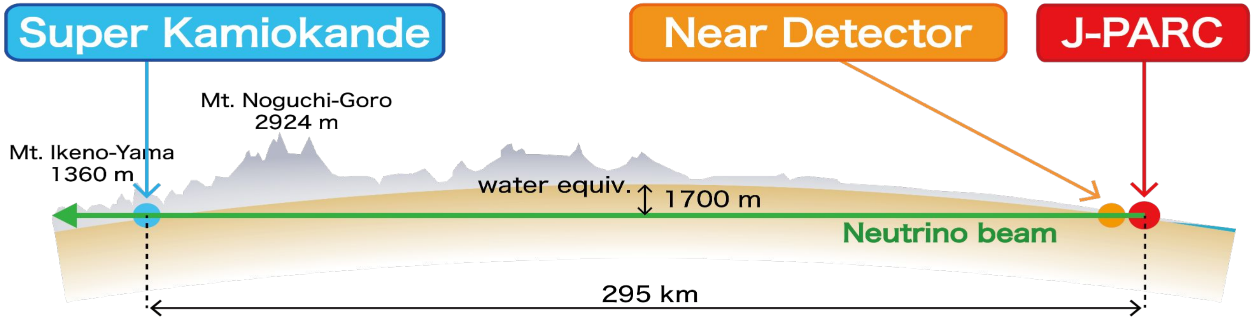

- Studies the neutrino oscillations of accelerated neutrinos
- High intensity **~600 MeV** ν_μ or $\bar{\nu}_\mu$ beam produced at J-PARC
- Neutrinos detected at Near Detector (**ND280**) and at the Far Detector (**Super-Kamiokande**)

Physics Goals

- Observation of ν_e and $\bar{\nu}_e$ appearance to determine $\boldsymbol{\theta_{13}}$ and $\boldsymbol{\delta_{CP}}$
- Precise measurement of $\boldsymbol{\theta_{23}}$ and $|\Delta m^2_{32}|$ through ν_μ and $\bar{\nu}_\mu$ disappearance

T2K Near Detector Complex

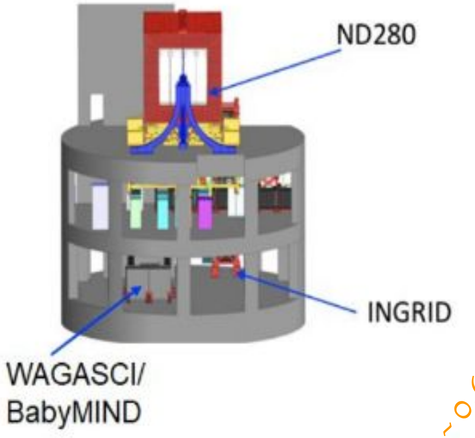

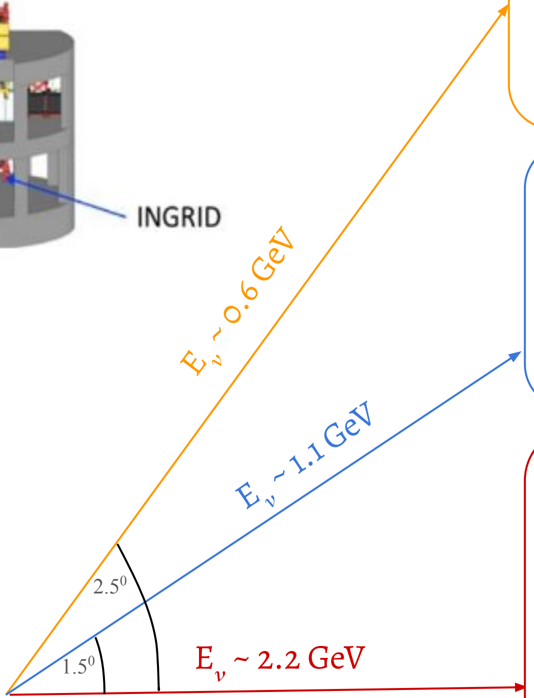

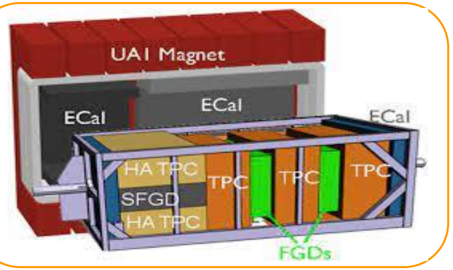

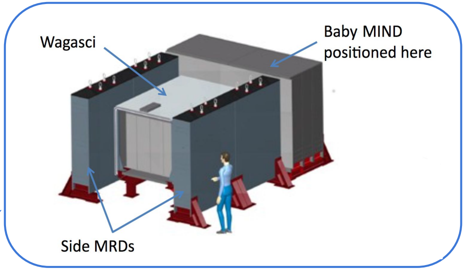

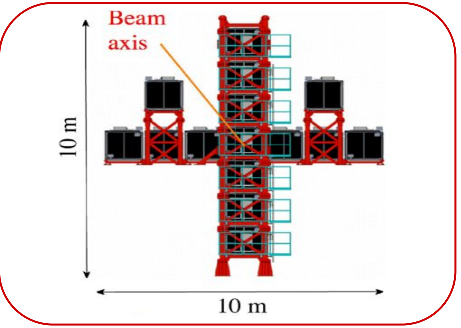

muon
neutrino

ND280 Detector

Constraints systematics in T2K oscillation analysis
Beam characterisation before oscillation
Measure neutrino cross-sections
Neutrino interaction studies
In operation since 2010, upgraded in 2023

WAGASCI-Baby MIND

Water Grid And SCIntillator detector to measure neutrino interaction cross-sections on water
Baby Magnetized Iron Neutrino Detector to identify charge and momentum of muons produced in neutrino interactions

INGRID

Interactive Neutrino Grid is in operation since 2009
Monitor neutrino beam profile day-by-day
Measure neutrino interaction rates

Upgraded ND280 arXiv:1901.03750

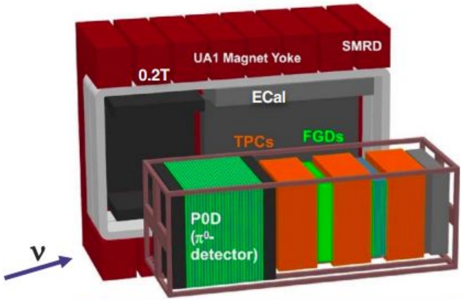

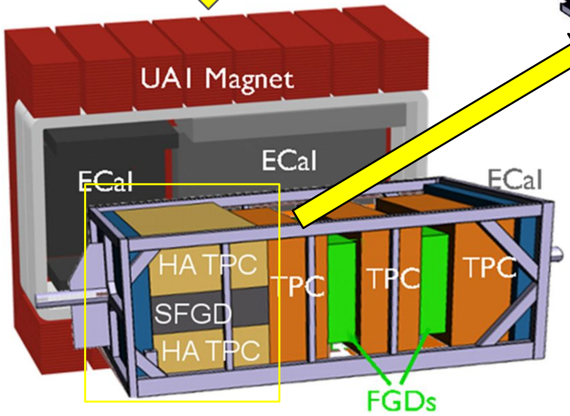

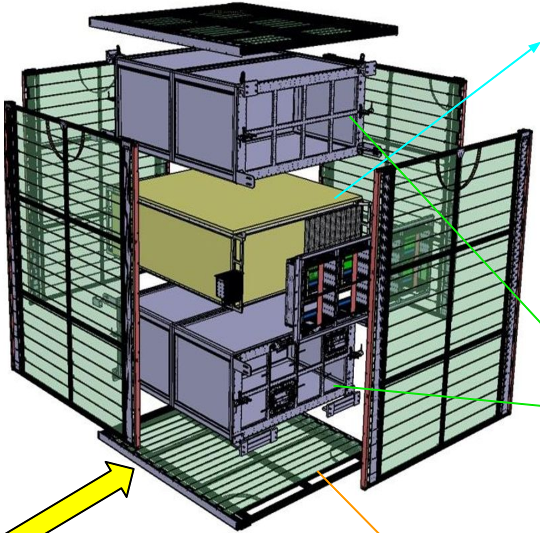

Super Fine-Grained Detector (SFGD) arXiv:1707.01785

- Active neutrino target
- 3D grid of 2 million plastic scintillator cubes of 1 cm³.
- Excellent resolution to reconstruct proton & Neutrons will be reconstructed

2 High-Angle TPC (HA-TPC) arXiv:1907.07060

- Novel lightweight composite field cage
- Readout using resistive micromegas
- 4π acceptance of charged particles & enhanced particle tracking

6 Time-of-Flight Detector (ToF) arXiv:2109.03078

- Measure arrival time of particles with a precision of ~150 ps
- Determine particle direction – whether it's incoming or outgoing
- Reject backward background (particles entering from outside)

HA-TPC Timeline

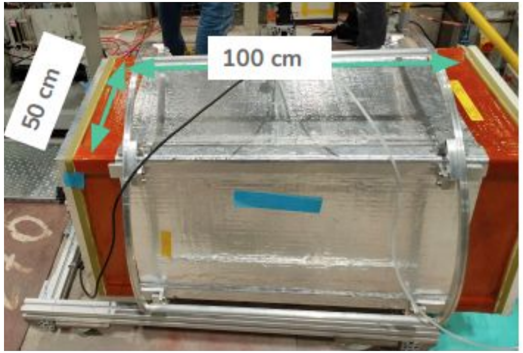

HA-TPC prototypes, tested with test beams at DESY & CERN
arXiv:2212.06541

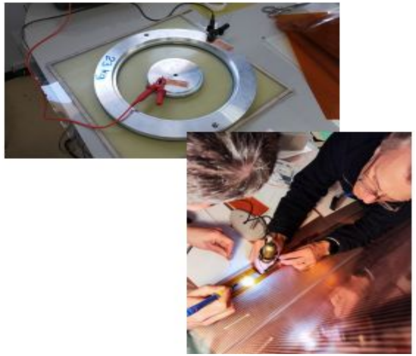

TPC prototype characterization
arXiv:1907.07060, arXiv:2106.12634

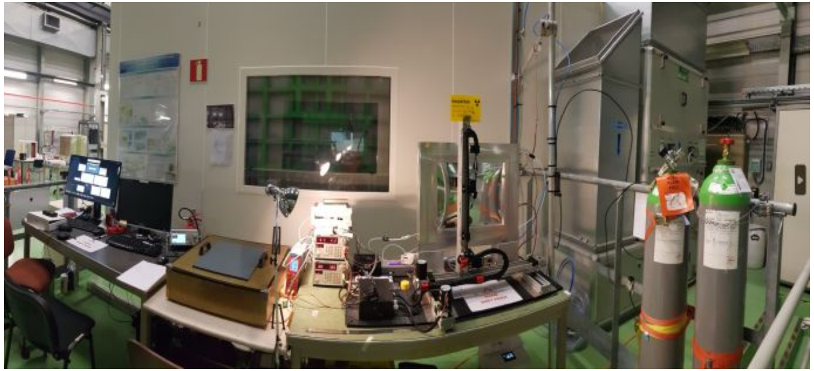

Characterization & validation of resistive micromegas with X-ray test bench at CERN arXiv:2303.04481

Bottom HA-TPC installed at J-PARC in September 2023

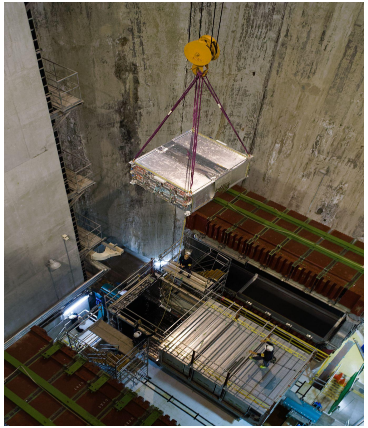

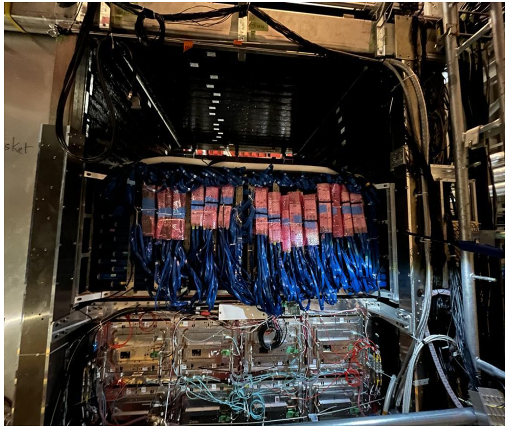

ND280 Upgrade Installation completed in May 2024

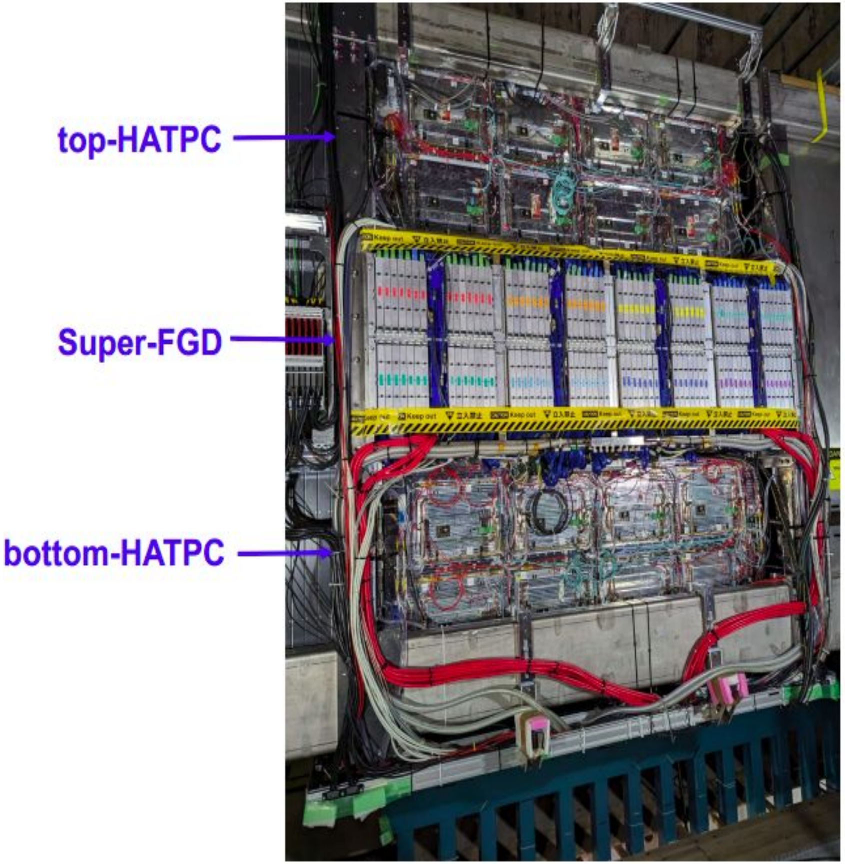

Neutrino Interaction from 1st run of full Upgrade

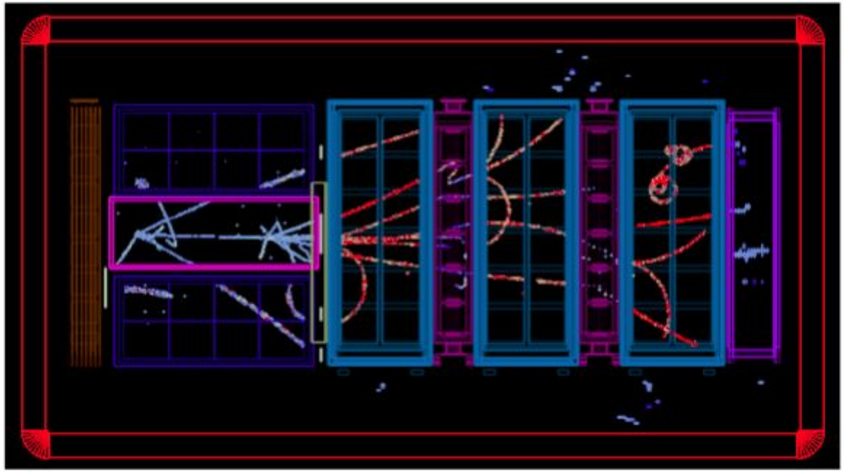

Talk by ***William Saenz*** on ND280 Upgrade

Talk by ***Lorenzo Giannessi*** on SFGD

Poster by ***Emanuele Villa*** on commissioning & performance of ToF

HA-TPC Specifications

1. **Momentum Resolution** $\sigma_p/p < 10\%$ at 1 GeV/c (Neutrino Energy)
2. **Energy Resolution** $\sigma_{dE/dx} < 10\%$ (PID muons & electrons)
3. **Space Resolution** O(500 μm) (3D tracking & pattern recognition)
4. **Low material budget walls** (matching track from neutrino active target)

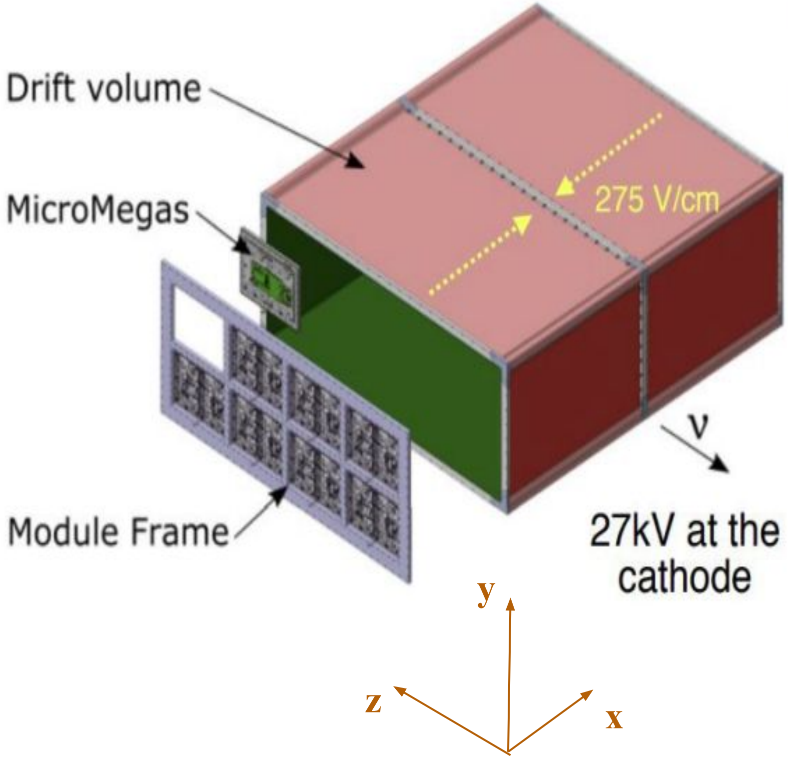

Atmospheric Pressure TPC

- Gas: **T2K mixture** (Ar:CF4:isoC4H10 = 95:3:2)
- Gas contaminants better than O(10 ppm) level
- Drift length **1 m**
- Central cathode at **-27 kV**
- E field uniformity $< 10^{-3}$ at 15 mm from walls
- Active volume of the O(3 m^3)

Charge Readouts - ERAM

Resistive layer enables charge spreading

- Space resolution below 500 μm with larger pad of cm size
- Less FEE channels → low cost
- Improved resolution at small drift distance (where transverse diffusion cannot help)

Resistive layer prevents charge build-up & quench sparks

- Enables operation at higher gain
- No need for spark protection circuits for ASIC → max active volume

Resistive layer encapsulated & properly insulated from GND

- Mesh at ground & resistive layer at +HV
- Improved field homogeneity → reduced track distortion
- Better shielding from mesh & DLC(Diamond Like Carbon) → potentially better S/N

Encapsulated Resistive MicroMegas

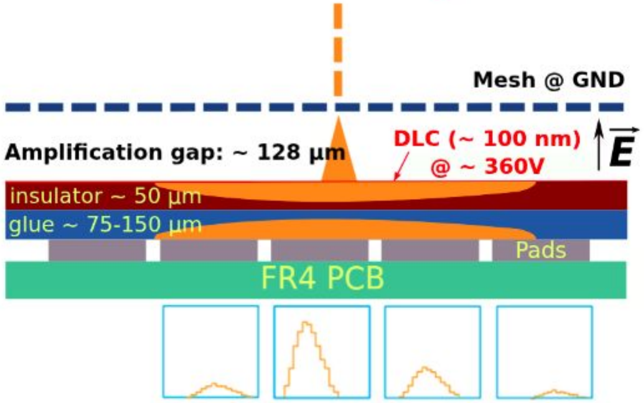

Final ERAM layout

- 36 x 32 pads
- Pads of 11.8 x 10.09 mm^2
- ~400 kΩ/❐ DLC resistivity
- 150 μm glue
- Overall active anode surface of the O(3 m^2)
- Sampling length ~ 60-160 cm
- 10k + 10k channels per TPC at EndPlates

Reconstruction Algorithm

MC Simulation

The position of the track is reconstructed based on the logarithm (ln) of the charge in the leading pad and in the neighboring pads

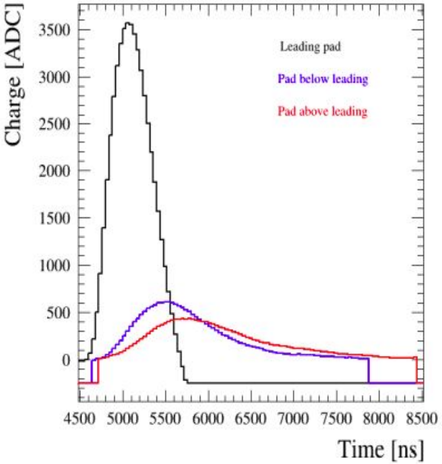

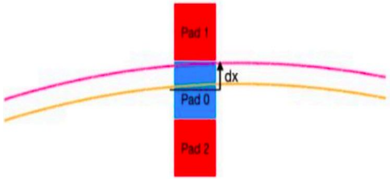

$dx = f(\log(Q_1/Q_0) \text{ or } \log(Q_2/Q_1))$

Q0: Charge on the leading pad
Q1: Charge on the 1st sub-leading pad
Q2: Charge on the 2nd sub-leading pad

Poster by [*Ulysse Virginet*]

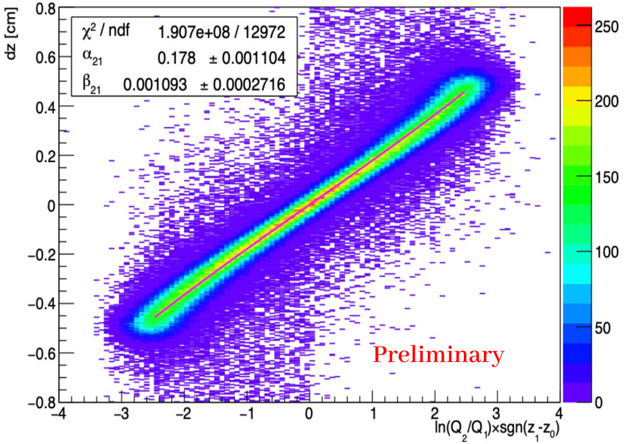

Track near the **center of the pad**, Q0 ≫ Q1 ~ Q2 & **ln(Q2/Q1) is informative**

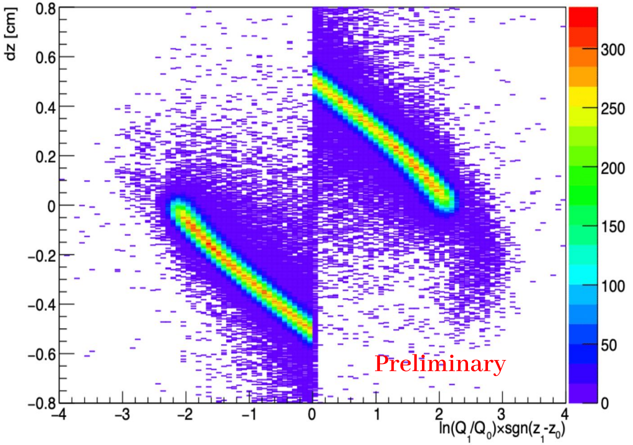

Track near the **edge between two pads**: Q0 ~ Q1 ≫ Q2 & **ln(Q1/Q0) is significant**

Performance of Reconstruction

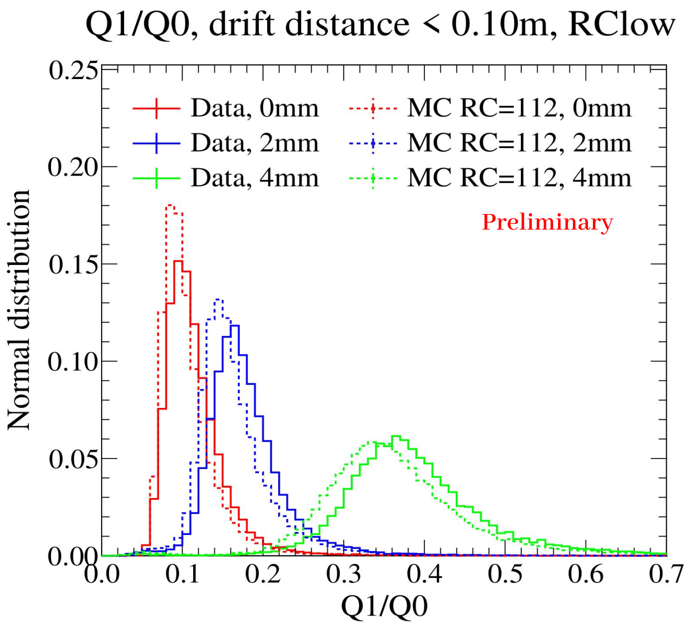

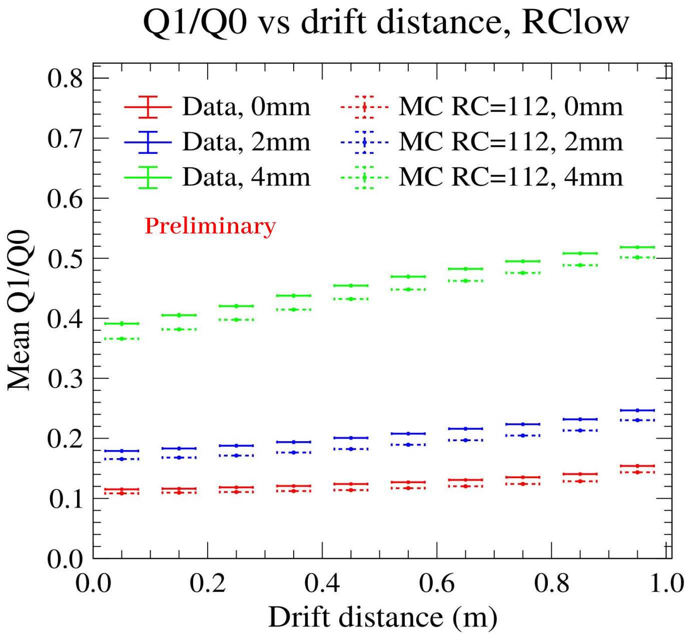

- ➔ Cosmic tracks with **z_{rec} - z_{centre} = 0 mm / 2 mm / 4 mm**, averaged per group of ERAM
- ➔ Small drift distances are considered to neglect diffusion effects
- ➔ Observed an overall **match MC simulation to cosmic data**, with a slight reduction from the simulations
- ➔ Underestimation persists throughout the drift region, more evident for tracks further from the leading pad

ERAM Alignment

1. Δz : The distance between both extrapolated segments at the middle of the inter-ERAM void
2. Δφ : The angle made by the extrapolated segments
3. φ : The angle made by the top segment with the horizontal
4. d > 0 : The lever arm
5. L, fixed : The inter-ERAM distance (typically 25 mm)

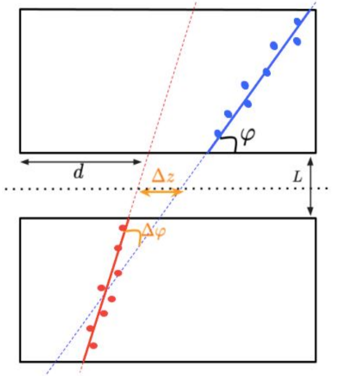

- Alignment performed using cosmic ray track without magnetic field
- Matched track segments from top & bottom ERAMs to determine misalignments
- Initial relative misalignment:
  Shifts of a few hundred μm
  Rotations of a few milliradians
- Residuals along the vertical axis:
  Before alignment: Large systematic deviations (±150 μm)
  After alignment: Residuals centered around zero
- The alignment procedure successfully corrected relative offset between ERAMS

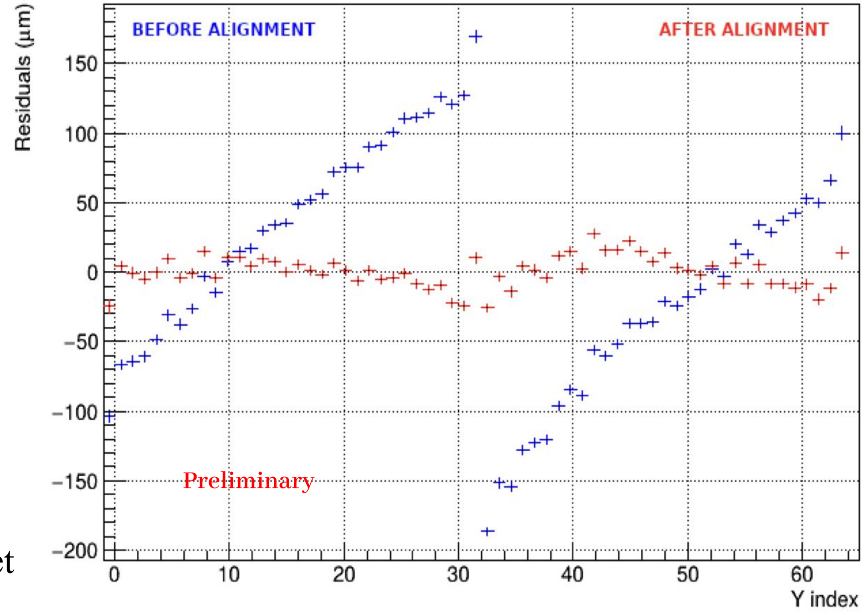

Electric Field Studies

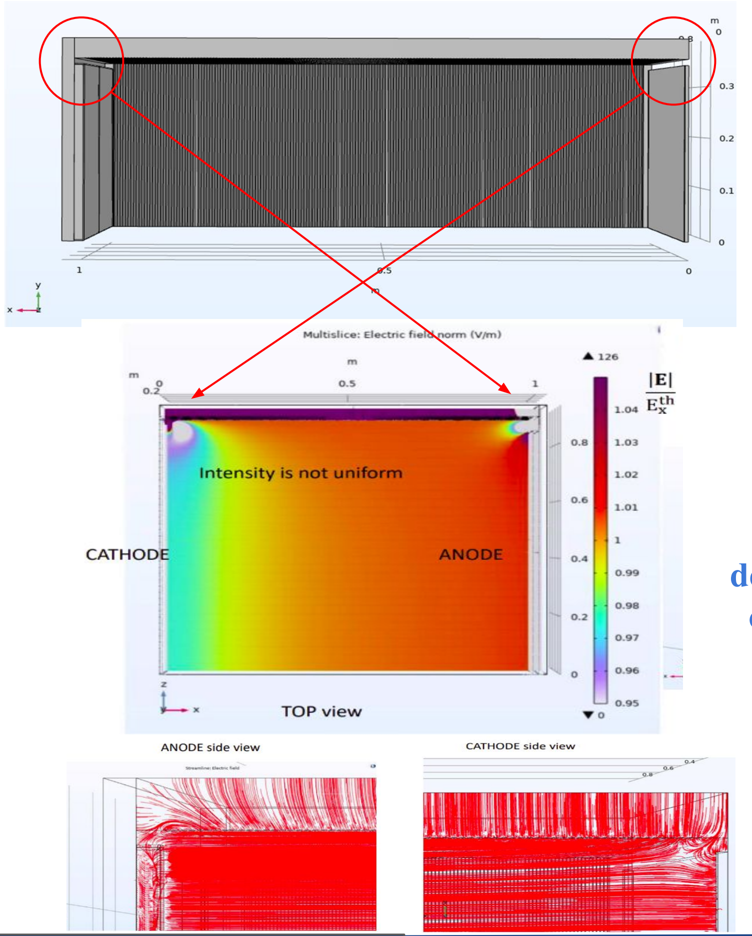

HA-TPC geometry has been integrated in COMSOL- Multiphysics

Numerical simulation of Electric Field

Detailed Electric field maps computed → integrated into reconstruction package

Electric field deformations on edges of both cathode and anode

Near the cathode: A large potential difference between the cathode and first strip and the external shielding

Near the anode: The whole ERAM surface is at ground, as well as the module frame; therefore, all the surfaces at the same potential are not placed in the same direction and at the same x value.

Electric Field Studies

Curvature distribution in bottom HA-TPC EndPlate 0

- Only cosmic data with NO B Field is considered
- Use “almost” vertical tracks in YZ plane

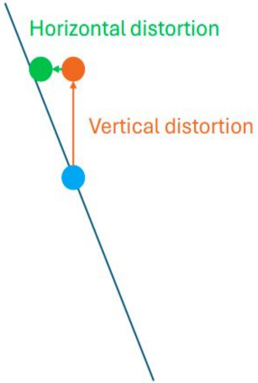

Fitted with a Gaussian distribution, and their centroid is estimated

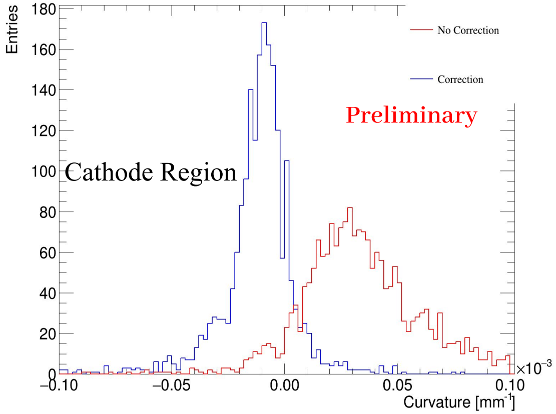

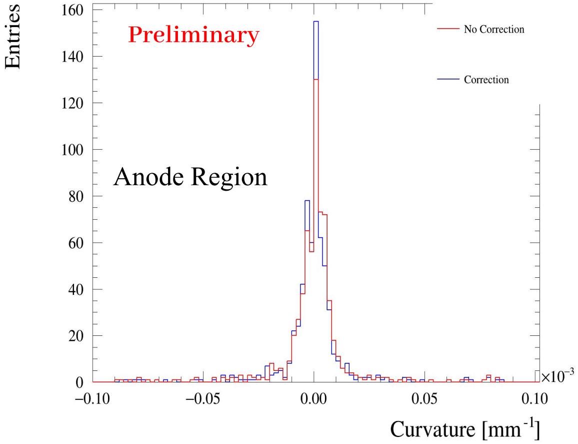

Curvature before & after E-field correction

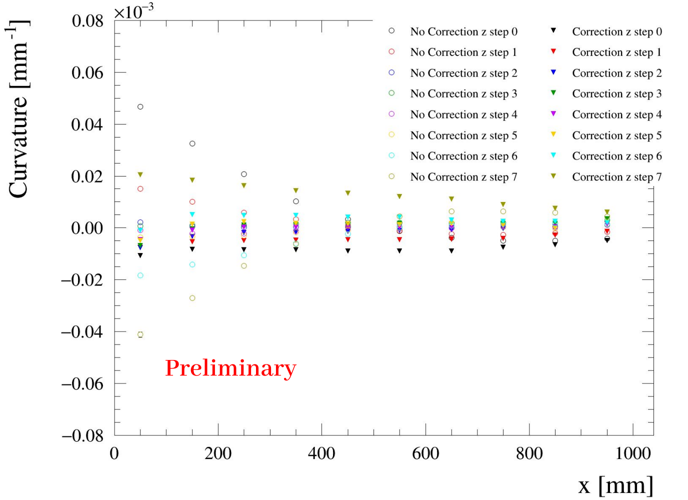

The inclusion of Electric field correction greatly reduces the magnitude of biases in the Cathode region

Spatial Resolution – YZ Plane

- Because of presence of the magnetic field, in YZ plane **track is curved**
- Final step of the reconstruction: **fitting the track with a helix**
- For each cluster along the track:

$$\text{residual} = \sqrt{(y^{\text{rec cluster}} - y^{\text{track fit}})^2 + (z^{\text{rec cluster}} - z^{\text{track fit}})^2} - R$$

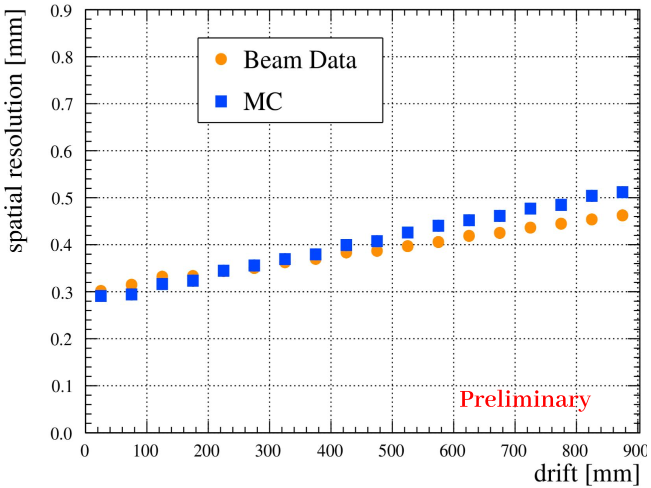

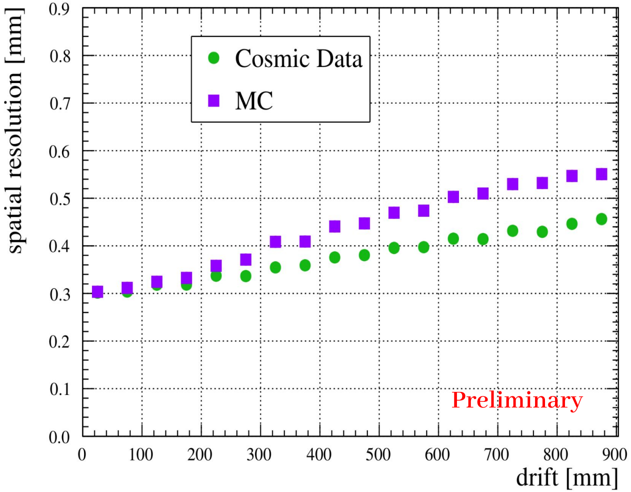

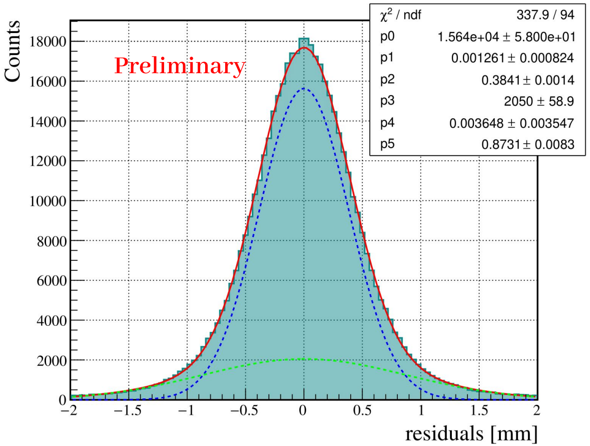

Distribution of residual from all track fitted with function corresponding to the convolution of two Gaussian distributions

$$\text{spatial resolution} = \frac{A_1\sigma_1 + A_2\sigma_2}{A_1 + A_2}$$

A_1 & A_2 : amplitude of 2 Gaussian peaks
σ_1 & σ_2 : standard deviation of 2 Gaussian

- The measured spatial resolution in the **beam data meets the performance requirement**
- For cosmic data, the agreement between data and MC simulation is less satisfactory (under investigation)
- In both beam and cosmic data, **spatial resolution is increasing with the drift distance**

Momentum Resolution

MC simulations were performed by generating vertical, diagonal, and horizontal tracks with a momentum of 1 GeV/c
The **standard deviation of Gaussian fit** is taken as the momentum resolution

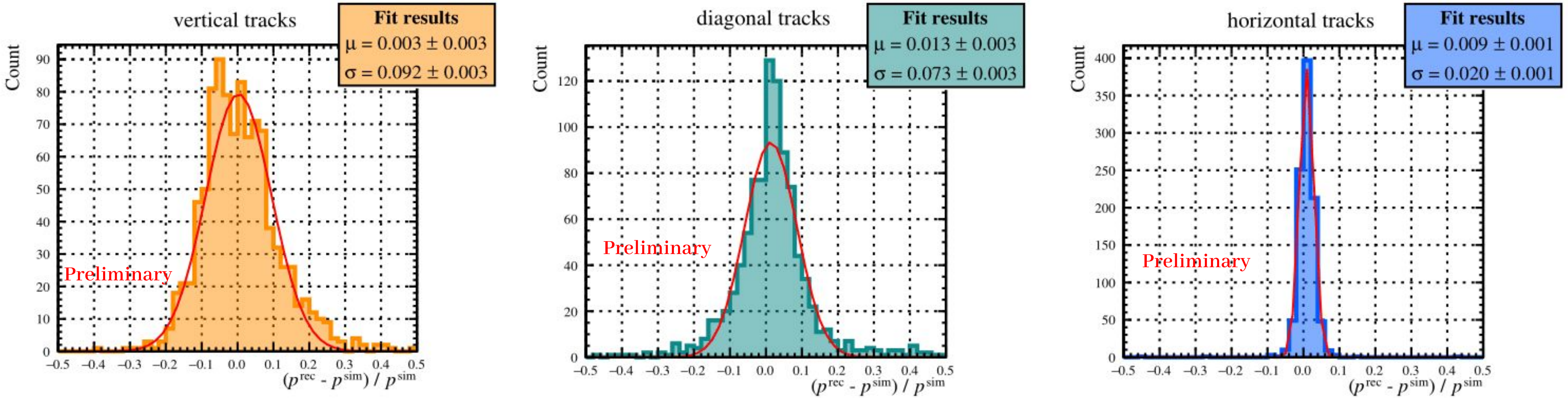

momentum resolution is 9.2% **momentum resolution is 7.3%** **momentum resolution is 2.0%**

Transverse momentum resolution is evaluated using;

$$\frac{\sigma_{p_t}}{p_t} = \sigma_{xy} \cdot \frac{p_t}{eBl^2} \cdot \sqrt{\frac{720}{N_p + 4}}$$

Longer tracks has better momentum resolution:

- ❏ horizontal tracks: average track length 1560 mm
- ❏ diagonal tracks: average track length 723 mm
- ❏ vertical tracks: average track length 621 mm

All three cases satisfy the target requirement of a momentum resolution better than 10%

The dE/dx

- The deposited charge per pad is inferred from a 2D diffusion model, using track angle, drift time & pad geometry
- dE/dx is computed as total inferred charge over total track length, after truncating pads with high local dE/dx.

Reconstructed dE/dx as a function of the reconstructed momentum for horizontal tracks

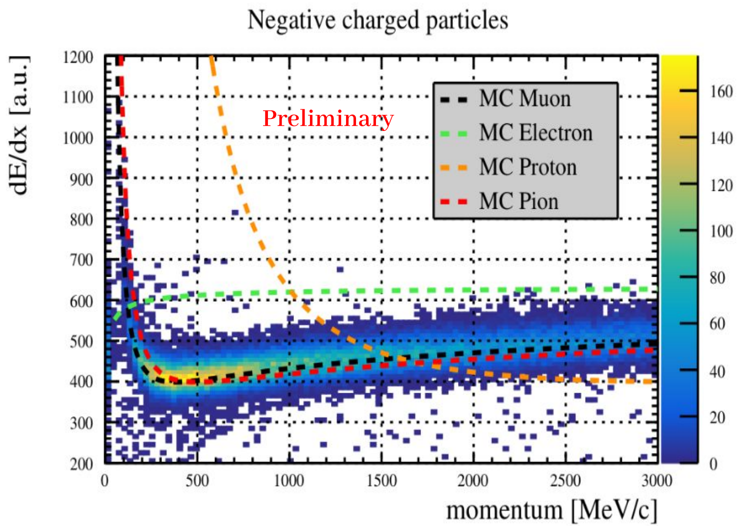

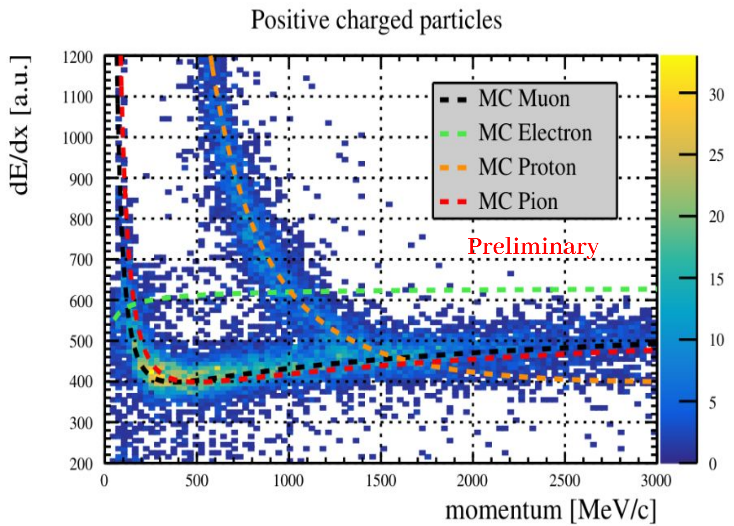

- The **muon band** is clearly visible in both plots
- **Protons** appear only in the plot for positive charged particle
- **electrons and positrons** populate the low-momentum region in both cases

dE/dx Resolution & PID

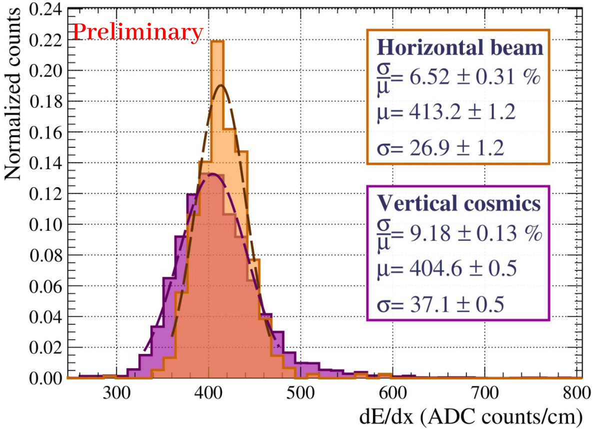

To get dE/dx resolution, data was binned with respect to the momentum

For each momentum slice, the bulk of the obtained distribution was fitted with a Gaussian

The resolution is then defined as **σ/μ**

The beam data has a dE/dx resolution of **6.52 ± 0.31%**, & cosmic data has **9.18 ± 0.13%**

dE/dx resolution as a function of the reconstructed momentum

Energy resolution on beam data varies between **6 and 7%** & **improving for larger momenta**

MC simulation follow the same trend, with a better resolution

dE/dx resolution as a function of the track length

The resolution improvement is **compatible with the expected 1/√L** trend

MC simulation matches the real data. It improves faster to reach a 1 point difference for the longest tracks

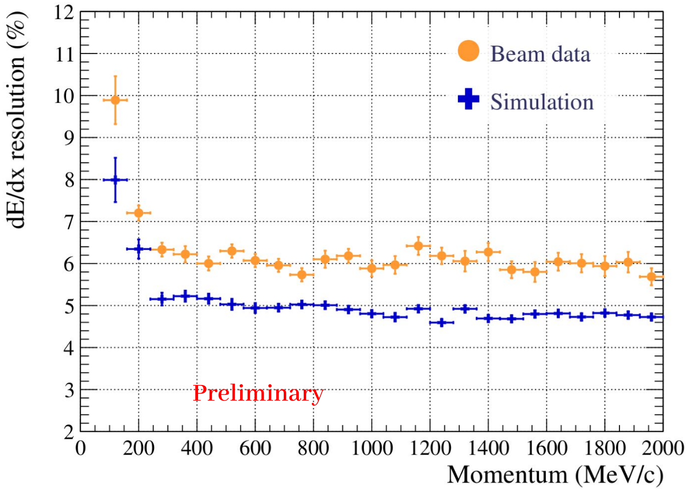

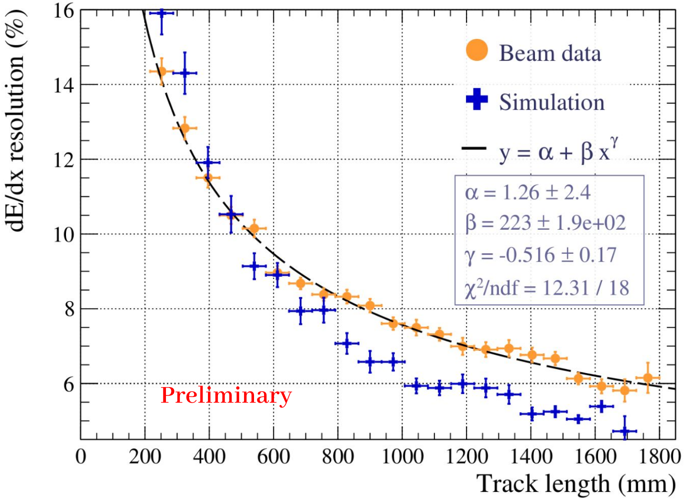

Spatial Resolution – YX Plane

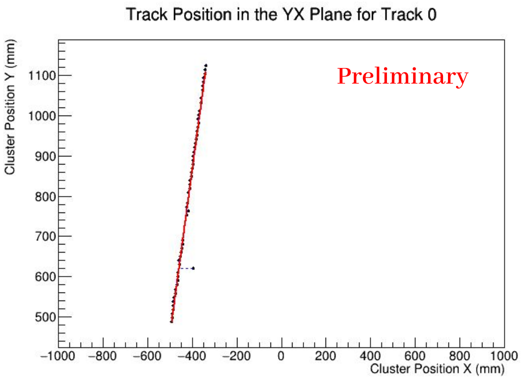

XY → Linear Track (with & without B field)

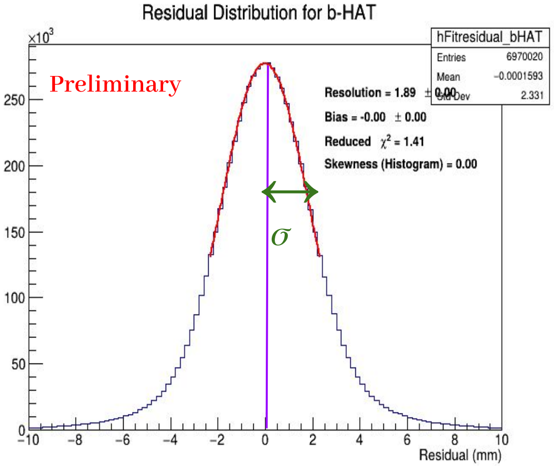

- The resolution has a **steep increase close to the cathode region**
- Resolution remain constant in middle of the field cage
- MC simulation overestimate the resolution

- The bias has higher values, which **peak very close to the cathode**
- The sign of the bias changes near the cathode, and both endplates have different signs
- MC simulation reproduce the general bias pattern in cosmic data, but with larger fluctuations at the edges

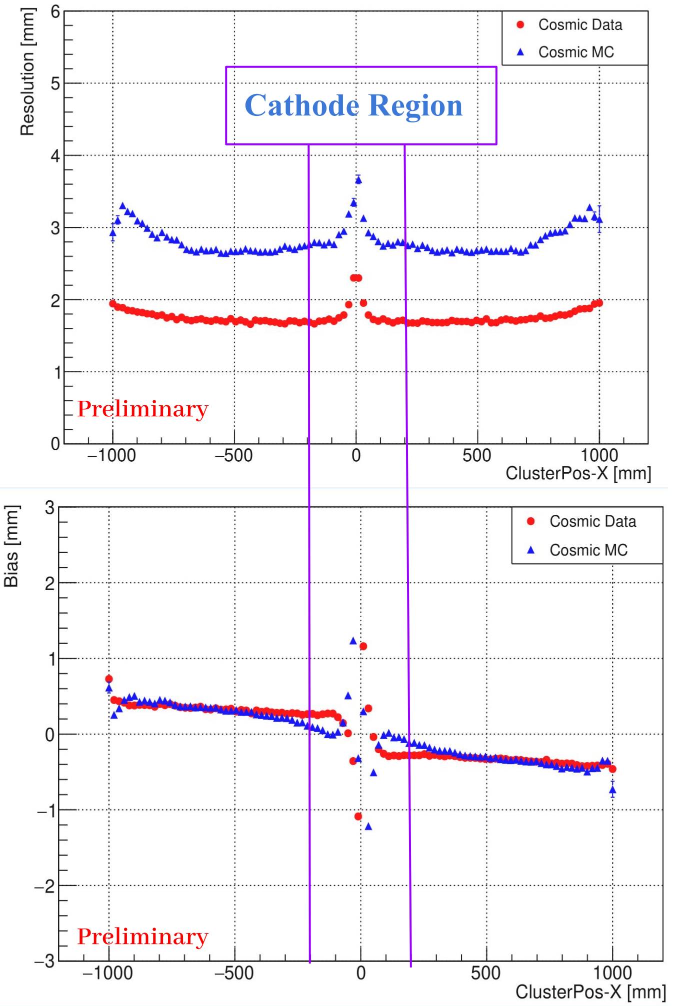

Hyper-Kamiokande Experiment

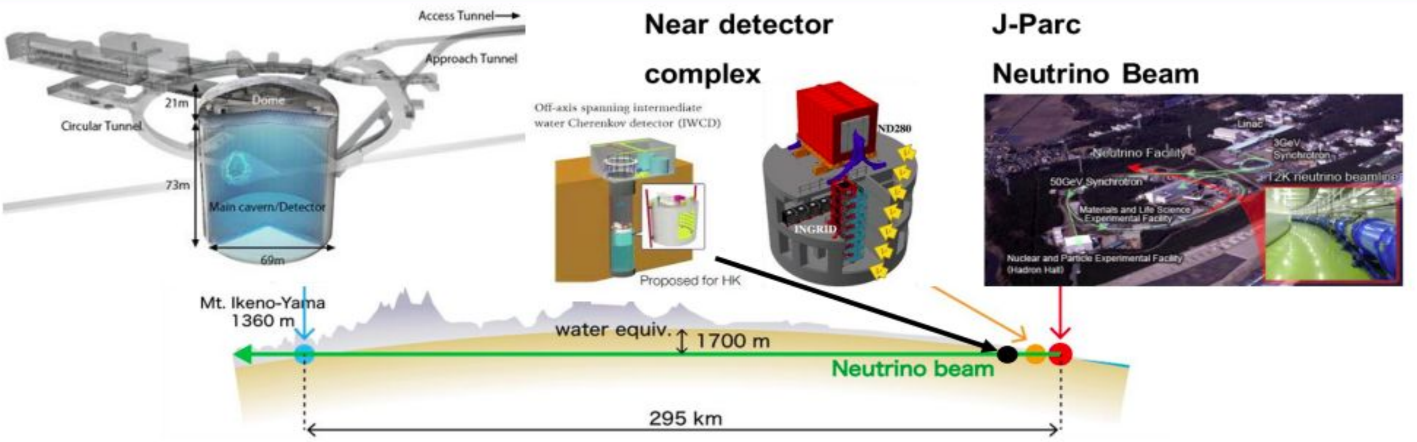

- **ND280 Upgrade including HA-TPC, continues as near detector for Hyper-K**
- New subdetectors will replace the TPCs and FGDs from old ND280
- Replace Super-K with a new Far Detector: ~8 times the fiducial mass of Super-K
- ND280 is complemented by the new Intermediate Water Cherenkov Detector (IWCD), located 1–2 km from the beam

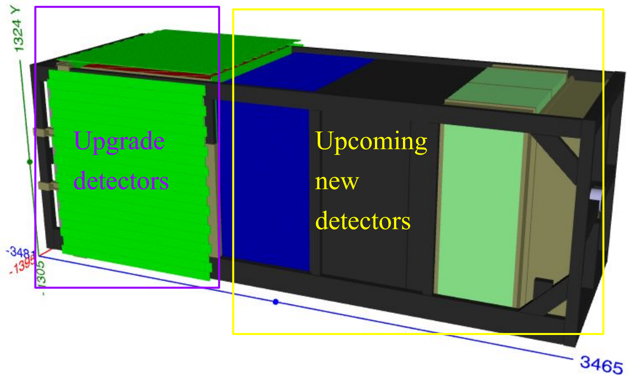

Summary

The **ND280 Upgrade** has been successfully completed.

The HA-TPC **operations are smooth**.

The performance of HA-TPC **fulfils the physics requirements**.

A **new paper on HA-TPC performance** is in preparation to submit in NIM-A journal.

HA-TPC will continue its operation in the **Hyper-Kamiokande experiment**.

Contents

THANK YOU

Back-Up

Limitations of ND280

Muons at ND280
Forward Region

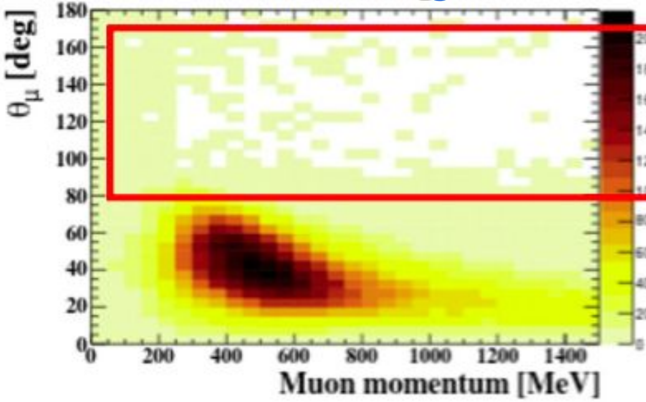

Electrons at Super-K
4π acceptance

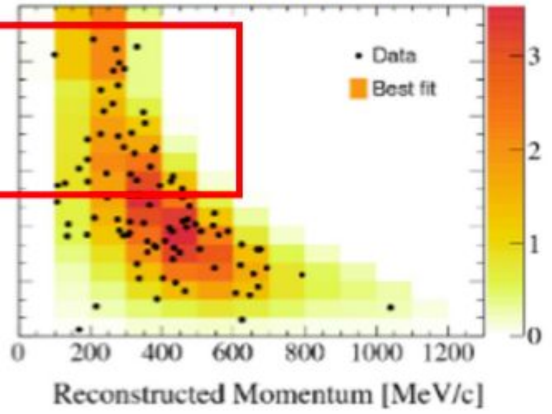

Proton Detection Efficiency

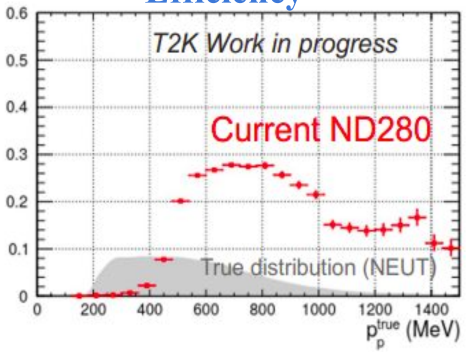

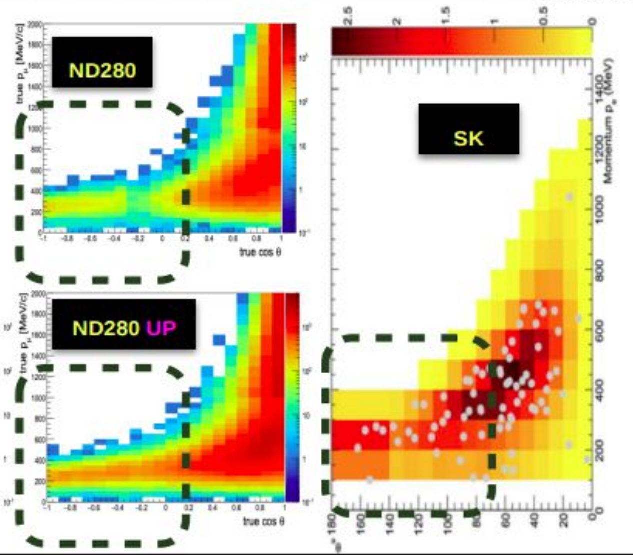

- Limited acceptance for particles with large scattering angle
- Low efficiency to track low momentum protons
- No neutron information
- Poor electron/photon separation for ν_e measurements
- Limited ToF information resulting in out-of-fiducial-volume background

Improvements with Upgrade

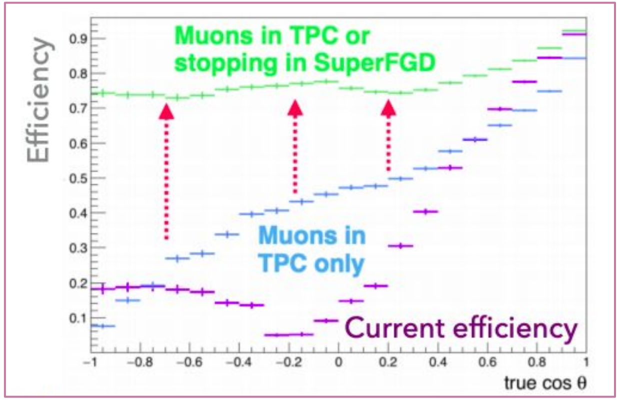

1. HATPC allows to reconstruct high angle charged particles exiting SFGD
2. SFGD allow the full reconstruction of 3D tracks issued by ν interaction - Lower threshold & excellent resolution to reconstruct protons at any angle (Proton threshold down to 300 MeV/c)
3. Neutrons reconstructed by using time of flight between vertex of ν interaction and neutron scattering
4. Better separation between γ and e from ν_e interactions

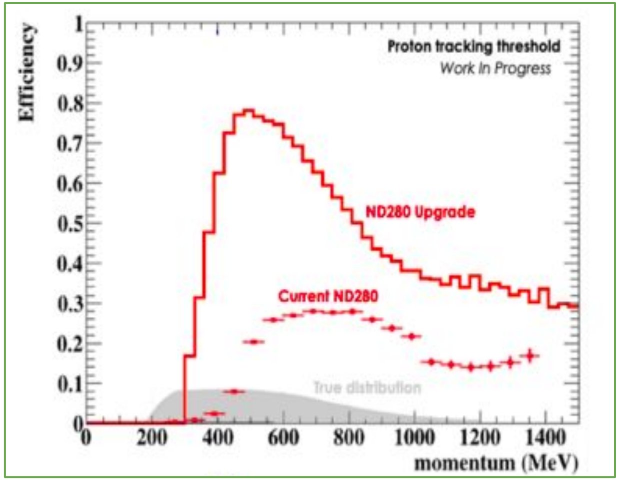

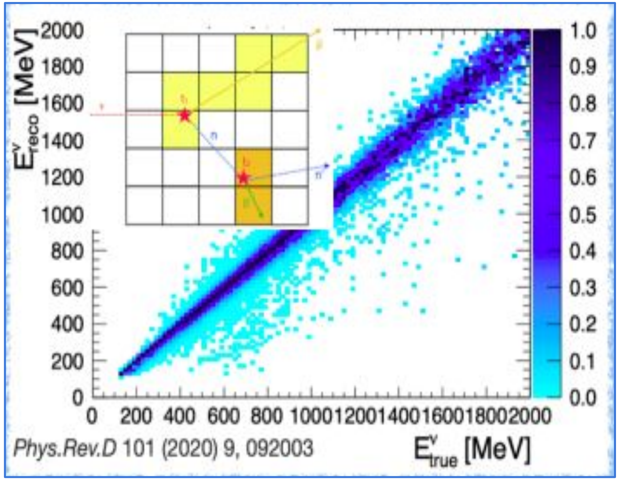

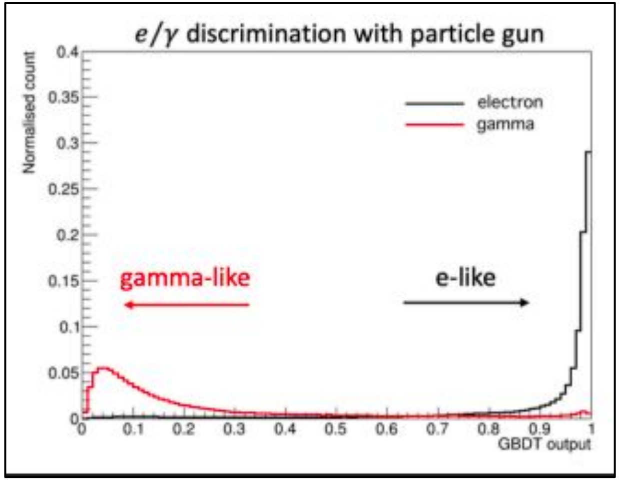

Field Cage for HA-TPC

Cathode

8 ERAMS

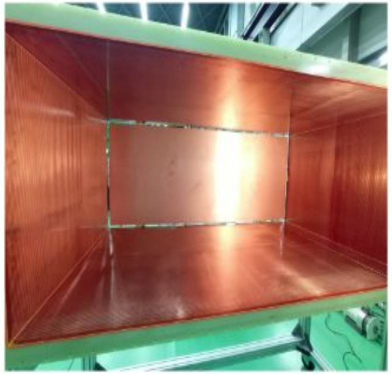

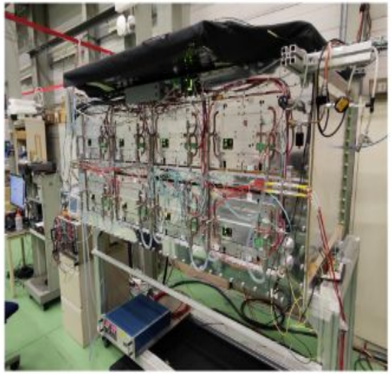

Cross-section of wall

- ❑ Field Cage → thin & low density walls
- ❑ Made up of composite materials
- ❑ Minimize dead space & maximise tracking volume

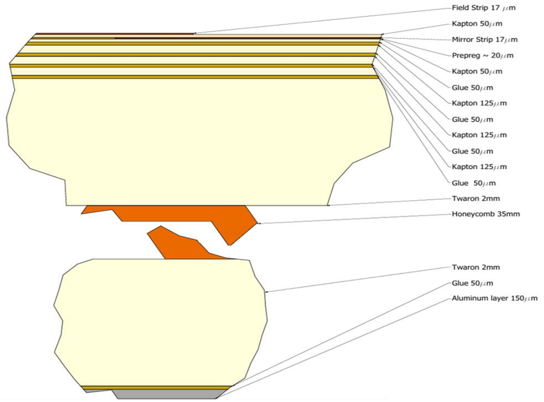

strip width 3 mm & pitch 5 mm

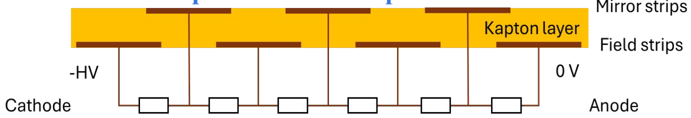

- Innermost part of FC → shape Electric field from cathode to anode
- Double layer of copper strips on kapton foil
- Two voltage dividers connect alternatively “field”-”mirror” strips 5 MΩ resistors & overall resistance of 1 GΩ

ERAM Production

Crucial Steps

- Selecting DLC foil resistivity
  -Large variation from DLC provider
  -Value stable after annealing
- Gluing Steps
  -DLC to PCB
  -Stiffner to DLC-PCB

Finalised PCB

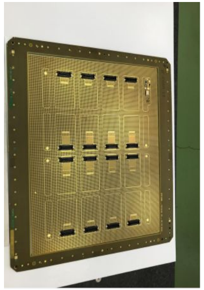

Stiffener

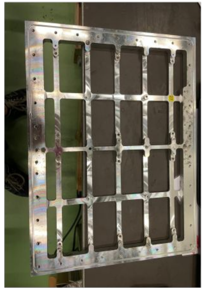

Setup for gluing of the PCB onto the stiffener

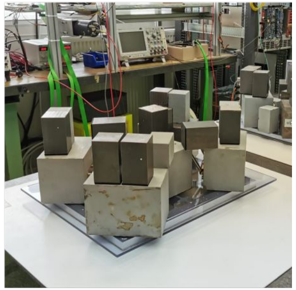

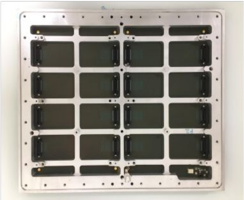

Assembled ERAM

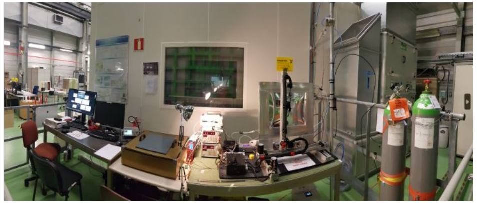

Qualification test setup at CERN

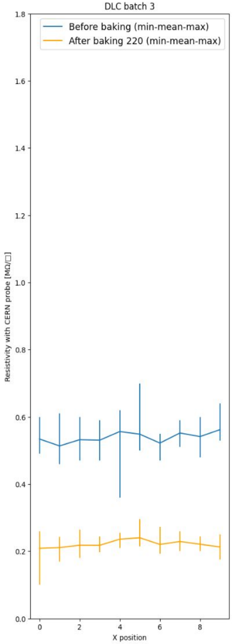

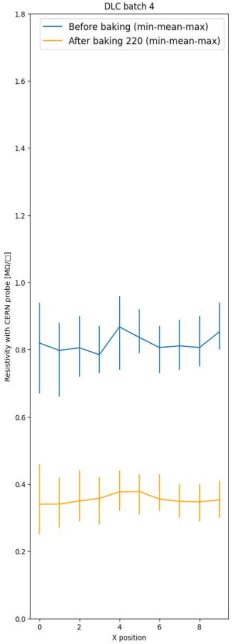

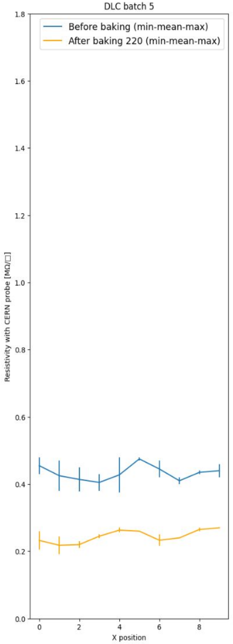

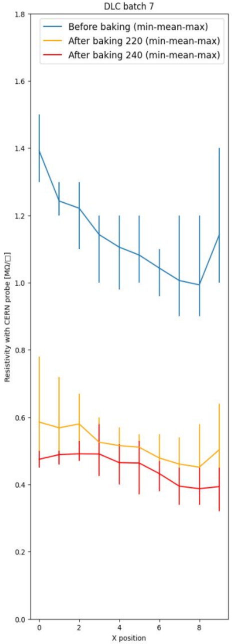

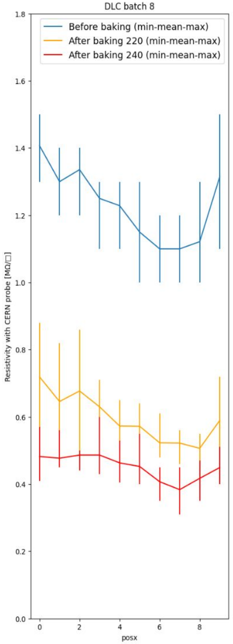

ERAM Performance

For each detector, the RC, gain and energy resolution measured in each pad from test bench scan

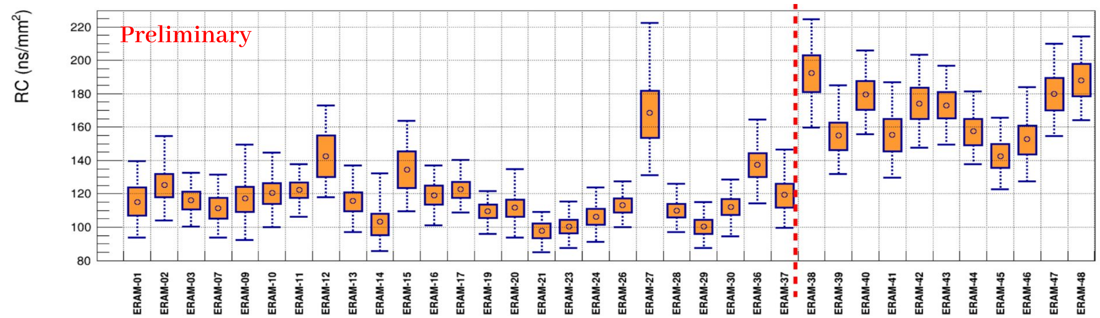

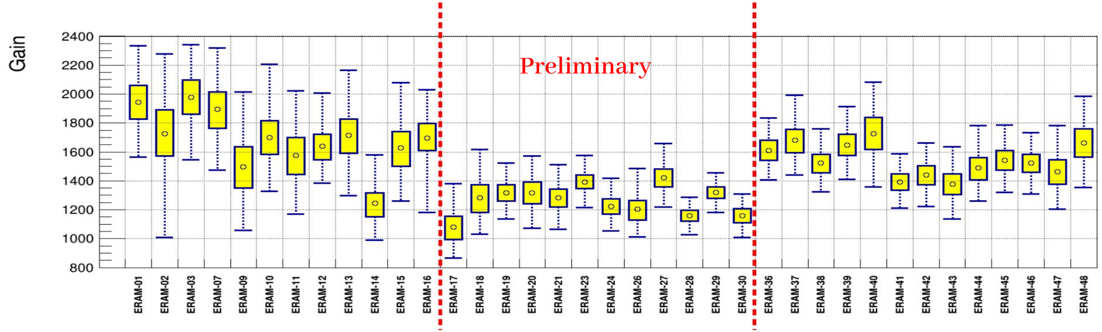

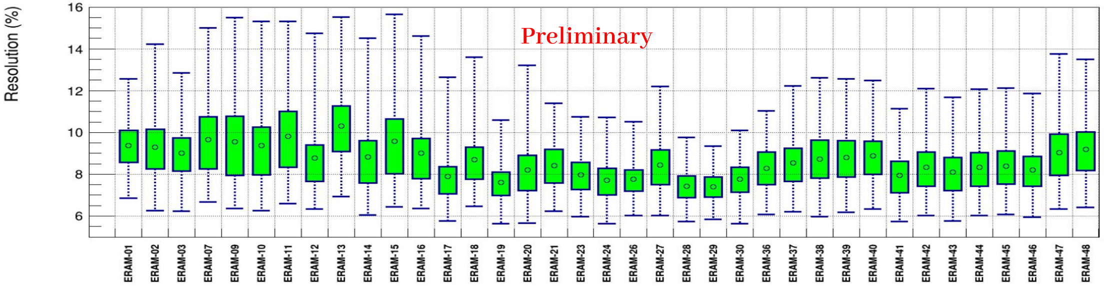

RC values depend on batch of DLC foils used - from ERAM 38, last batches of DLC & has higher surface resistivity

For the gain 3 production periods

- Till ERAM-16 large spread - extra solder mask & copper layers caused local compression of gap
- Between ERAM-17 & ERAM-30 reduced gain - removal of the solder mask layer and replacement of the plain copper grounding layer
- From ERAM-36 large gain - gap thickness reduced

- Energy resolution very consistent throughout the production of the detectors
- The spreading of the values is larger for the detectors produced before ERAM-17 - presence of the soldermask layer
- Spread reduced after the removal of soldermask layer

Gas System

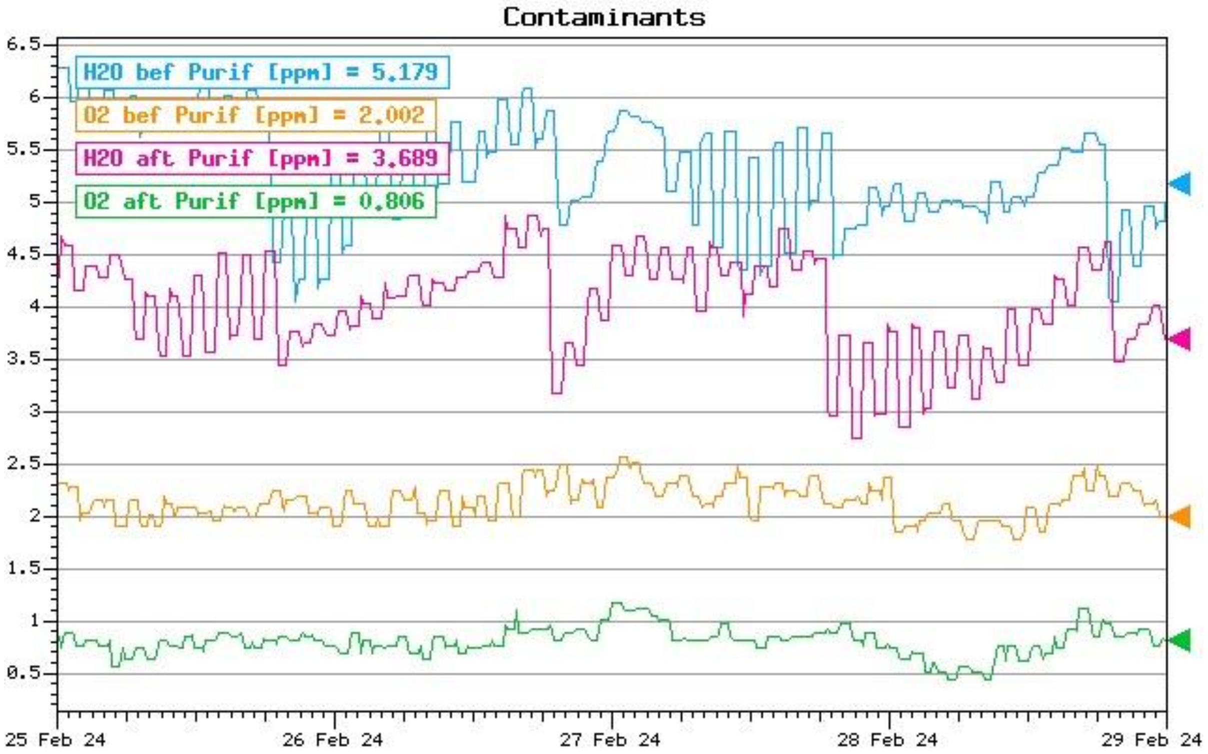
Contaminants
H2O bef Purif [ppm] = 5.179
O2 bef Purif [ppm] = 2.002
H2O aft Purif [ppm] = 3.689
O2 aft Purif [ppm] = 0.806
6.5
6
5.5
5
4.5
4
3.5
3
2.5
2
1.5
1
0.5
25 Feb 24
26 Feb 24
27 Feb 24
28 Feb 24
29 Feb 24

Gas Monitoring System

Schematic overview of the GMCs used for monitoring the drift gas

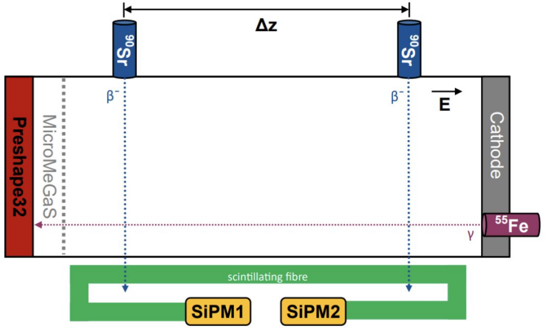

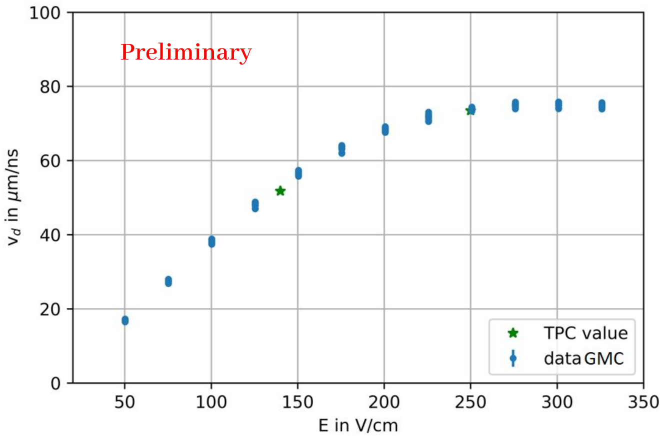

HA-TPC drift velocity measurements agree with GMC scan, confirming accurate gas condition monitoring

Monitoring results for drift velocity

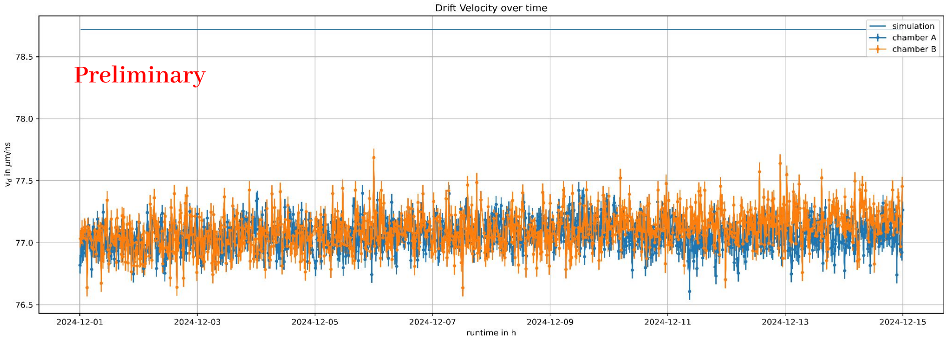

A small difference between the measured true drift velocity and the simulation for the ideal gas mixture

Monitoring results for gain

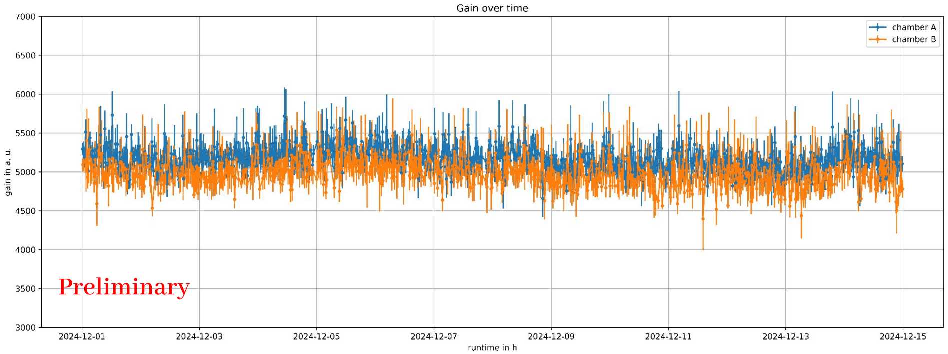

the measured gain no time variations were observed, showing a constant gas quality

HAT Simulation

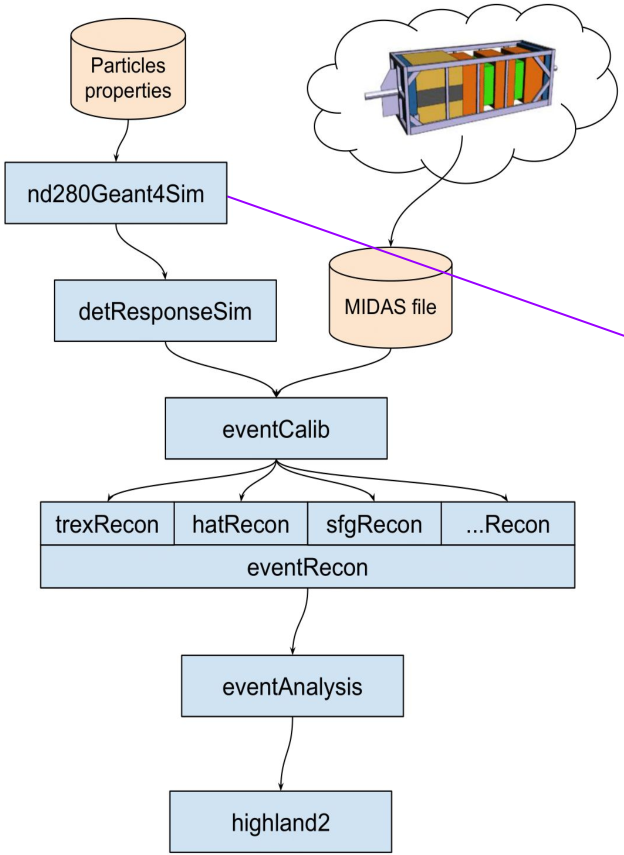

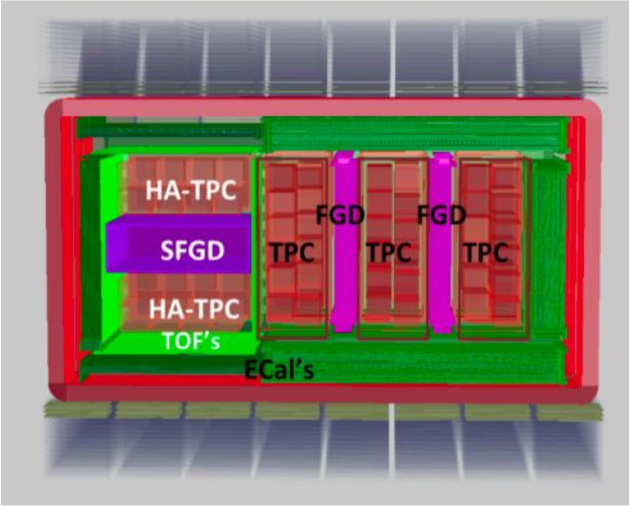

- ND280 Geometry has implemented
- COSMOL simulated B field map with non-zero B_y & B_z components
- Simulation of neutrino interactions/lepton track particle gun

HAT Simulation

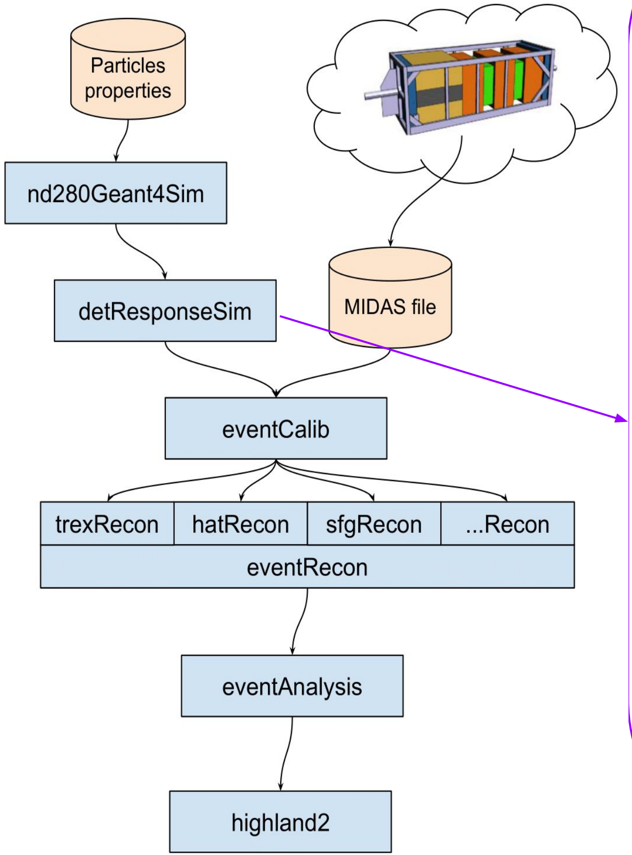

- Ionization electron's drift to the ERAM plane simulated with the Langevin equation:

$$\vec{V}_d = \frac{\mu}{1+(\omega\tau)^2}\left(\vec{E} + (\omega\tau)\frac{\vec{E}\times\vec{B}}{|\vec{B}|} + (\omega\tau)^2\frac{(\vec{E}\cdot\vec{B})\vec{B}}{|\vec{B}|^2}\right)$$

- e^- showers simulated with Polya distribution:

$$P_m(g) = \frac{m^m}{\Gamma(m)}\cdot\frac{1}{G}\left(\frac{g}{G}\right)^{m-1}\exp\left(-m\frac{g}{G}\right)$$

- Charge spreading on the ERAM plane:

$$\rho(\vec{r},t) = \frac{RC}{4\pi t}\times\exp\left(-\frac{r^2RC}{4t}\right)$$

- The unit waveform is then the convolution of the unit charge with the time derivative of the electronics response:

$$WF_{\mathrm{unit}}(t) = Q_{\mathrm{unit}}(t) * \frac{dE}{dt}(t) = \int_{-\infty}^{\infty} Q_{\mathrm{unit}}(t-\tau)\frac{dE}{d\tau}(\tau)\,d\tau$$

HAT Reconstruction

Hits preparation: waveforms are transformed into hits to obtain Qmax & Tmax

Pattern recognition: merging individual hits using the TRex algorithm into pattern

Merging: track merging between the different ERAMS and/ or endplates

Clustering: logQ method to reconstruct position in each cluster & helix fit performed on those reconstructed positions

Particle Identification: based on the combined measurement of the momentum and the dE/dx

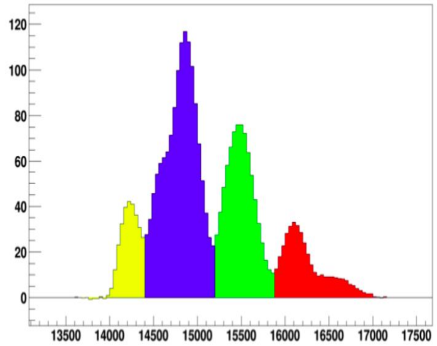

- Each color corresponds a new waveform or hit pad object
- Charge of a hit: the maximum of the waveform

The TREx pattern recognition algorithm is based on A* path-finding algorithm

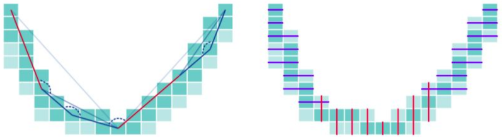

- 3 goodness of fit are evaluated: One obtained from the fit of each individual pattern (χ_1^2 and χ_2^2), and the other one corresponding to the combined pattern χ_J^2
- The 2 patterns are merged together if,

$$\chi_J^2 < 1.3 \times \sqrt{\chi_1^2 \times \chi_2^2}$$